Journal of Materials Chemistry A

Accepted Manuscript

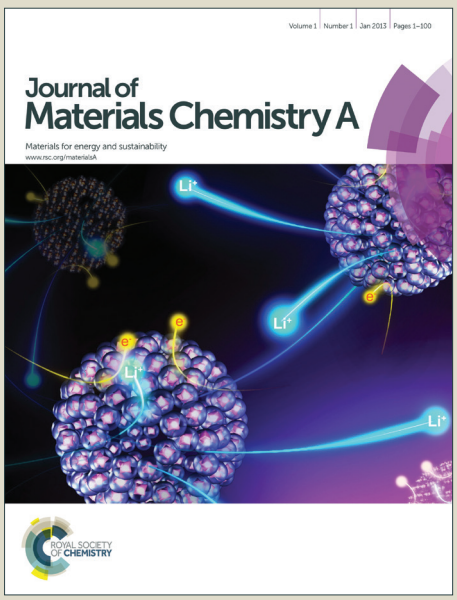

ROYAL SOCIETY OF CHEMISTRY

www.rsc.org/materialsA

A New Layered Sodium Molybdenum Oxide Anode for Full Intercalation-Type Sodium-ion Batteries

Kai Zhu,[ab] Shaohua Guo,[a*] Jin Yi,[a] Songyan Bai,[a] Yingjin Wei,[b*] Gang Chen[b] and Haoshen Zhou[a,c*]

a Energy Technology Research Institute, Institution National Institute of Advanced Industrial Science and Technology (AIST), Umezono 1-1-1, Tsukuba, Japan

b Key Laboratory of Physics and Technology for Advanced Batteries (Ministry of Education), College of Physics, Jilin University, Qianjin Street 2699, Changchun, China

c National Laboratory of Solid State Microstructures & Department of Energy Science, Nanjing University, Nanjing 210093, China

*Corresponding author: guo.shaohua@outlook.com; yjwei@jlu.edu.cn; hs.zhou@aist.go.jp

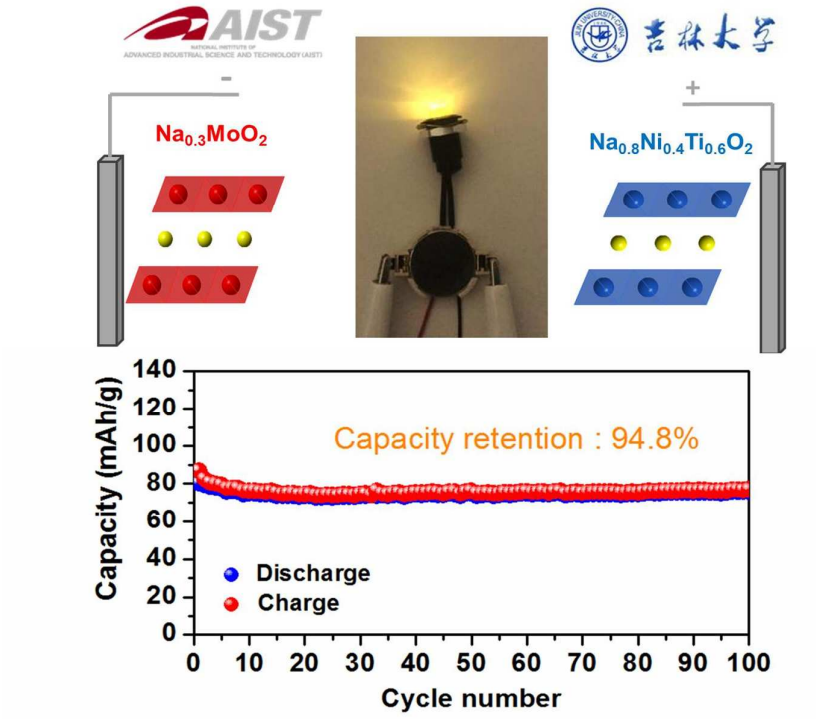

Abstract: A new layered $Na_{0.3}MoO_2$ exhibits a reversible capacity of 146 mAh/g, remarkable cycling stability and good rate capability for sodium half-cell. And a $Na_{0.3}MoO_2$ // $Na_{0.8}Ni_{0.4}Ti_{0.6}O_2$ full intercalation-type sodium-ion cell is fabricated and it displays an excellent cycling stability. These results indicate molybdenum-based oxide is a promising anode material for sodium-ion batteries.

Journal Name

COMMUNICATION

A New Layered Sodium Molybdenum Oxide Anode for Full Intercalation-Type Sodium-Ion Batteries

eceived 00th January 20xx,
Accepted 00th January 20xx

DOI: 10.1039/x0xx00000x

www.rsc.org/

Kai Zhu,[ab] Shaohua Guo,[a*] Jin Yi,[a] Songyan Bai,[a] Yingjin Wei,[b*] Gang Chen[b] and Haoshen Zhou[a,c *]

A new layered $Na_{0.3}MoO_2$ exhibits a reversible capacity of 146 mAh/g, remarkable cycling stability and good rate capability for sodium half-cell. And a $Na_{0.3}MoO_2$ // $Na_{0.8}Ni_{0.4}Ti_{0.6}O_2$ full intercalation-type sodium-ion cell is fabricated and it displays an excellent cycling stability. These results indicate molybdenum-based oxide is a promising anode material for sodium-ion batteries.

In the past decades, wind and solar energies, as a sustainable electricity generation, become a promising alternative to the traditional fossil fuel.[1] Due to the nature of these renewable energy sources and the requirement of smart grid management, a large-scale energy storage system is extremely necessary to realize the transfer of electrical energy from peak to off-peak periods.[2] Although lithium-ion batteries (LIBs) have gained a huge success in the portable electronic devices and (hybrid) electric vehicles, they are not suitable for large-scale energy storage because of the increasing cost and limited resources of lithium.[3] Thus sodium-ion batteries (SIBs), as a potential alternative to LIBs, attract increasing attention for next generation large-scale energy storage system, on account of sodium's high abundance and low cost.[4]

Recently, many great works have made progresses in exploring capable cathode materials, such as layered transition metal oxides, tunnel-type $Na_{0.61}Ti_{0.48}Mn_{0.52}O_2$,[5] NASICON-structured $Na_3V_2(PO_4)_3$[6] and prussian blue[7]. However, only a few anode materials are available for SIBs. Therefore, developing favorable anode materials has become a key issue for the application of SIBs. There are three types of anode reactions for SIBs, which are categorized by their working principles, i.e. Intercalation type, conversion type and alloying type.[2] Although a large capacity of more than 500 mAh/g could be obtained through the conversion reaction or alloying process.[2,8-12] The large volume expansion/contraction is a big obstacle for their applications in SIBs, as the case in LIBs. Thus the intercalation anode materials become the best choice.[13] Hard carbon, as a typical intercalation material, exhibits a reversible capacity of 240 mAh/g at a voltage window of 0.01-2.0 V.[14] Unfortunately, the low sodium insertion voltage plateau at 0.1 V results in potential safety issue. Until now, the most of the intercalation-type anodes are titanium-based materials, which could provide a safe and low potential (Ti^{3+}/Ti^{4+}) relative to the Na^+/Na redox couple.[13, 15, 16] Shen et al. reported that $Na_2Ti_6O_{13}$ could display a high capacity of 196 mAh/g by lowering the cutoff voltage to around 0.0 V, which would lead to poor capacity retention of 73% after 30 cycles.[16] Yu et al. prepared layered $Na_{2/3}Co_{1/3}Ti_{2/3}O_2$, which could exhibit excellent cycle stability with a capacity under 100 mAh/g.[13] For these titanium-based materials, either low capacity or poor cycling retention cannot meet the requirement of the large scale energy storage system.

The advantage of low cost, abundant resources and non-toxic makes molybdenum-based materials seem to be another smart choice as well as the titanium-based anode. Furthermore, some molybdenum-based materials, such as MoS_2 or MoO_3, have shown good electrochemical performance for SIBs.[17, 18] However, it is a challenge to develop molybdenum-based materials as intercalation-type electrode for SIBs. Herein, a novel molybdenum-based material, $Na_{0.3}MoO_2$, is synthesized by a simple solid-state reaction, and it presents remarkable electrochemical properties as an anode material for SIBs at room temperature for the first time. A reversible discharge capacity of 146 mAh/g is obtained at a current density of 20 mAh/g with average voltage of 0.8 V in SIBs. Meanwhile, it exhibits remarkable rate ability and capacity retention. To further confirm the application of the materials, we fabricated a $Na_{0.3}MoO_2$ // $Na_{0.8}Ni_{0.4}Ti_{0.6}O_2$ full intercalation-type sodium-ion battery, which can buffer the volume change (cathode expanding companied with anode shrinking almost equally and vice versa). Moreover, the safety concern would be greatly improved due to high potential of 0.8 V in $Na_{0.3}MoO_2$. The full cell displays an

[a] Energy Technology Research Institute,Institution National Institute of Advanced Industrial Science and Technology (AIST) E-mail: guo.shaohua@outlook.com; hs.zhou@aist.go.jp
[b] Key Laboratory of Physics and Technology for Advanced Batteries (Ministry of Education), College of Physics, Jilin University. E-mail: yjwei@jlu.edu.cn
[c] National Laboratory of Solid State Microstructures & Department of Energy Science, Nanjing University.

Electronic Supplementary Information (ESI) available: Experiment details, dQ/dV curves, discharge-charge profiles and *ex situ* XRD pattern and linear fitting of I_p vs. $v^{1/2}$ relationship of $Na_{0.3}MoO_2$, rate ability of the full cell and charge-discharge curves of $Na_{0.8}Ni_{0.4}Ti_{0.6}O_2$ See DOI: 10.1039/x0xx00000x

excellent cycling stability and rate ability. Thus this molybdenum-based material might be a promising role as a new insertion anode for SIBs.

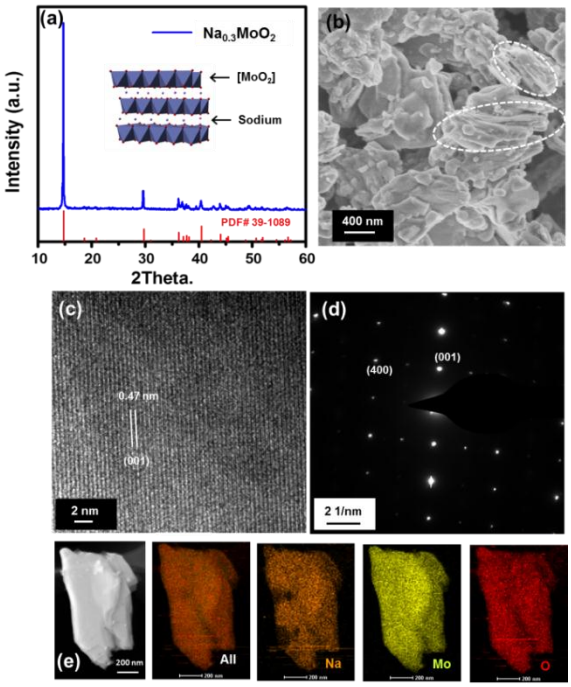

Figure 1. (a) XRD, (b) SEM image, (c) HRTEM image, (d) SAED pattern of the sample and (e) EDS analysis of the layered $Na_{0.3}MoO_2$. The inset of (a) is schematic of layered structure of $Na_{0.3}MoO_2$. White ellipses in (b) show the layered morphology of the samples.

The crystallographic structure of the $Na_{0.3}MoO_2$ compound is investigated by X-ray diffraction (XRD) as shown in **Figure 1a**. The peaks of as-prepared samples can be indexed to the monoclinic structure of $Na_{0.45}MoO_2$, which is consistent with the values from the standard card (PDF#39-1089). According to the Inductively Coupled Plasma (ICP) results, the mole ratio of the Na:Mo is 0.3:1, corresponding to a chemical composition is of $Na_{0.3}MoO_2$. The inset of **Figure 1a** shows the schematic of layered structure of $Na_{0.3}MoO_2$. The Na ions can be viewed as intercalated within the van der Waals gap of the [MoO_2] layer lattice.[19] The lattice parameters of samples are determined by the Celref program i.e. a=12.33 Å, b=2.88 Å and c=4.95 Å (90.0°×102.9°×90.0°). The morphology of $Na_{0.3}MoO_2$ is characterized by scanning electron microscopy (SEM) as shown in **Figure 1b**. The partials of the sample display typical layered morphology and their sizes range from 0.5-1 μm. And the detailed crystal structure of the layered $Na_{0.3}MoO_2$ is further characterized by transmission electron microscope (TEM). As shown in **Figure 1c**, the clear crystal lattices with a d-spacing of 0.47 nm corresponding to the (001) plane of $Na_{0.3}MoO_2$ are obtained. **Figure 1d** shows the SAED pattern of the material, which is indexed to the typical reflection originating from the layered structure. Moreover, the X-ray energy dispersive spectroscopy (EDS) analyses (**Figure 1e**) of $Na_{0.3}MoO_2$ present that the sodium, molybdenum and oxygen atoms are homogeneously distributed in the sample.

The electrochemical sodium storage properties of the $Na_{0.3}MoO_2$ are evaluated as anode material for SIBs. **Figure 2a** displays the typical discharge-charge profiles of the sample at a current density of 20 mA/g in the voltage range of 0.05-2 V. It can be observed that the $Na_{0.3}MoO_2$ electrode presents a safe average sodium ion insertion voltage of 0.8 V and delivers a reversible capacity of 146 mAh/g in the first few cycles. The reversible extraction corresponds to 0.7 sodium ion per $Na_{0.3}MoO_2$. It implies that sodium ion insertion into the [MoO_2] layer to form $Na_{0.3+x}MoO_2$ as illustrated in following Equation (1):

$$Na_{0.3}MoO_2 + xNa^+ + xe^- \rightarrow Na_{0.3+x}MoO_2 \qquad (1)$$

Meanwhile, in the initial discharge process, an irreversible capacity results in a low Coulombic efficiency, which may be ascribed

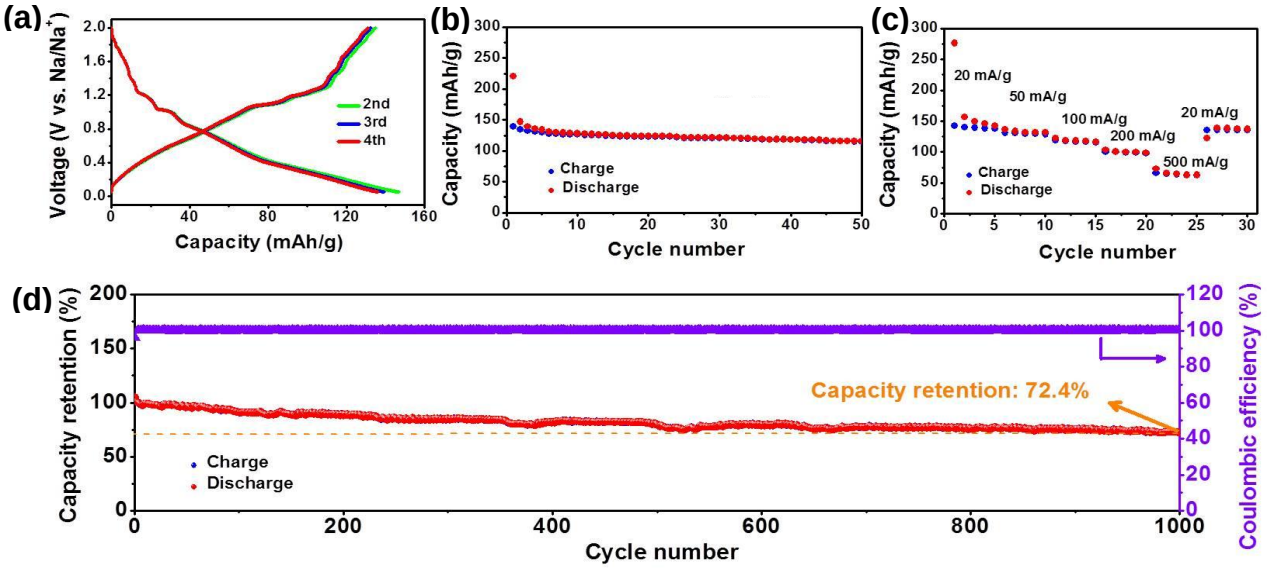

Figure 2. (a) galvanostatic discharge-charge curves and (b) cycling performance of $Na_{0.3}MoO_2$ in a voltage of 0.05-2 V at current density of 20 mA/g; (c) rate capability at various current rates; (d) long-term cycling performance at current density of 500 mA/g.

to the formation of the solid electrolyte interface (SEI) layer. The corresponding dQ/dV curves are given in the **Figure S1** and an irreversible peak located at 0.18 V appears in the initial discharge cycle, which could assign to the formation of the SEI.[11] Besides that peak, all other peak suggests complex and reversible reaction of Na insertion/extraction in the $Na_{0.3}MoO_2$ structure. Thus electrochemical insertion and deinsertion with the $Na_{0.3}MoO_2$ should proceed through several multiphase reactions, which is similar as other intercalation-type electrode materials for SIBs such as Na_xCoO_2 [20] and $Na_{0.44}MnO_2$ [21]. Furthermore, a stable cycle performance is shown as **Figure 2b** and it reveals good capacity retention of 85% after 50 cycles. Compared with other Ti-based anode materials, as-prepared $Na_{0.3}MoO_2$ material exhibits a much better electrochemical performance as shown in the **Table S1**.[13, 16, 22-24] In addition, *ex-situ* XRD patterns after the first cycle is recorded in comparison with the pristine one as shown in **Figure S3**. Though some minor unclear diffraction peaks appear, the main peaks of layer $Na_{0.3}MoO_2$ structure is retained. It suggests that the structure is reversible after sodium insertion and extraction. The unclear peaks may come from the SEI or some phase change under the voltage of 0.05-2 V.[12, 16] To further understand the structural changes during the Na extraction, *ex-situ* XRD patterns at different charge depths of the first cycle are investigated as shown in right of **Figure S4.** Upon the extraction of the sodium ion, the main (200) peak shifts towards lower angles indicating a-axis is expanding. Moreover, in the *ex-situ* XRD patterns obtained from the fully discharged electrode (as shown in **Figure S5**), the remaining peaks reflect ordering of cation ion within the layer intersites maintaining the layered structure and no peaks belonging to Mo metal or NaMo alloys are detected, which further confirm the multiphase reactions mechanism. Due to the low valence state of Mo is sensitive to the O_2, some impurity such as $Na_2Mo_2O_7$ are formed during the XRD testing in the air environment. It should be noticed that in the $Na_{0.3}MoO_2$, the Mo is in mixed valence of Mo^{3+} and Mo^{4+}. During sodium ion insertion, there may be a single-electron redox process of the Mo^{4+}/Mo^{3+} in the materials to form $NaMoO_2$, in which the Mo is in the valence of Mo^{4+}. Thus the sodium ion intercalation would induce lattice distortion, which leads to complex phase change.[13,15] It suggests that the structural evolution at the anode side should be multistep phase transition based on the reversible sodium insertion and extraction in layered Na_xMnO_2 structure. **Figure S6** presents the discharge-charge curves of $Na_{0.3}MoO_2$ at various current densities from 20 mA/g to 500 mA/g. When the current density is increased, the discharge voltage decreases and the charge voltage increases due to the polarization effect. Even so, the plateaus could still be distinguished. In addition, the rate dependent cycling performance is shown as **Figure 2c**. The reversible discharge capacities of 149, 133, 118, 100 and 65 mAh/g are obtained at current densities of 20, 50, 100, 200 and 500 mA/g, respectively. When the current density comes back to 20 mA/g, the discharge capacity returns at 138 mAh/g, which suggests structural stability of material. Moreover, the long-term cycling performance is further investigated for 1000 cycles at a current density of 500 mAh/g in the voltage window of 0.05-2 V as shown in **Figure 2d**. An excellent capacity retention of 72.4 % is obtained after 1000 cycles, which corresponds to a capacity fading of 0.028% per cycle. Meanwhile, a high Coulombic efficiency around 100% is maintained during the whole cycling process except for the the initial cycles.

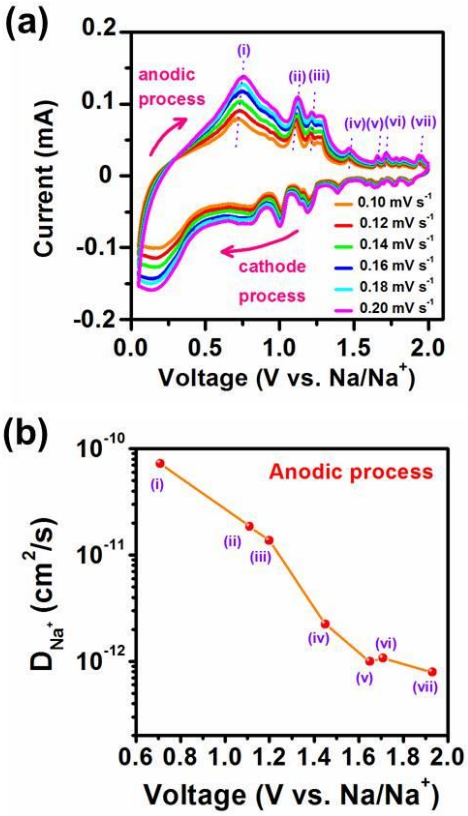

Figure 3. (a) CV curves of the $Na_{0.3}MoO_2$ at different voltage scan rate; (b) Diffusion coefficients of Na^+ in layered $Na_{0.3}MoO_2$ at different charge states

To further investigate the structure stability after 1000 cycles, the *ex-situ* XRD results are confirmed as shown in **Figure S3**. It could be found that the intensity of XRD peaks become weak and the crystallinity decreases, which is caused by complex reversible insertion/desertion of sodium ions during the long cycling. Even so, the main peaks of $Na_{0.3}MoO_2$ are maintained, indicating the good structure stability after the long cycling. In addition, it should be noticed that no carbon or metal oxide coating is carried out in this case, although literature reported that the surface modification could enhance the capacity and reversibility. Therefore, the layered $Na_{0.3}MoO_2$ material presents promising applications in sodium ion batteries due to its good cycle ability.

To further investigate the electrochemical kinetics of the $Na_{0.3}MoO_2$, the cyclic voltammetry (CV) has been used to determine the Na^+ diffusion coefficients (D_{Na}) of the material according to Equation (2).[25]

$$I_p = 2.69 \times 10^5 n^{3/2} S D^{1/2} v^{1/2} C \quad (2)$$

where n is the number of electrons per specific reaction, for Na^+ it is 1; S is the surface area of the electrode which is 1.53 cm^2 in this work; C is the concentration of Na ions in the material, I_p is the current intensity and v is the scan rate. At relatively low scan rates sodium ions accumulate in the active material thus I_p varies linearly with $v^{1/2}$ as shown in **Figure S7**. Based on this, the sodium diffusion coefficients can be calculated using the equation (2) and the results are shown in **Figure 3b**. Obviously, the sodium ion diffusion coefficient of the layered sodium molybdenum oxide trends towards decrease during the anodic process. This implies that the diffusion of Na^+ in the Na_xMoO_2 become increasingly difficult, which

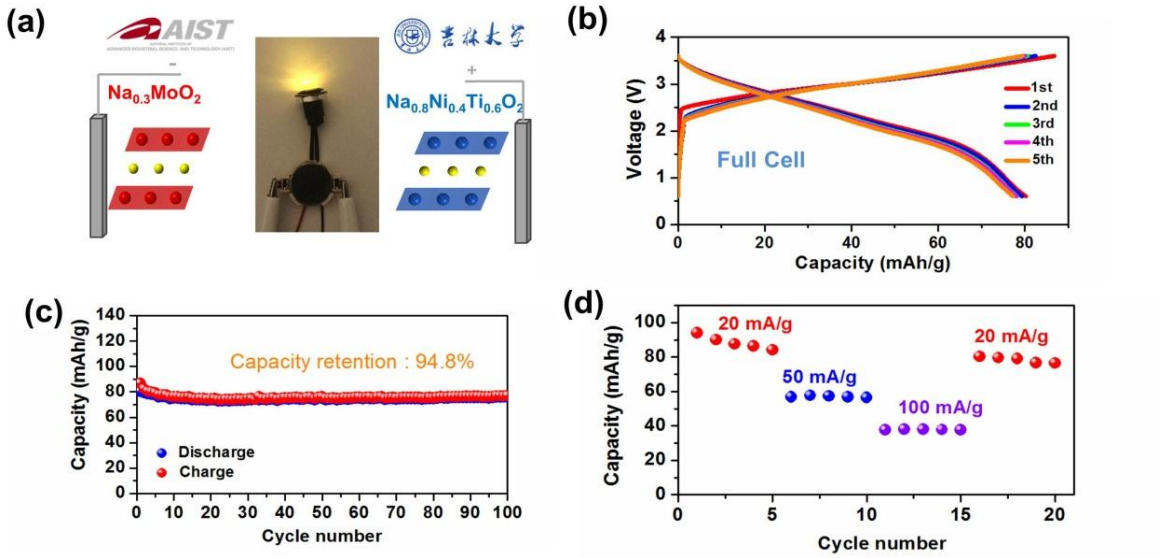

Figure 4 (a) A diagram of $Na_{0.3}MoO_2$ // $Na_{0.8}Ni_{0.4}Ti_{0.6}O_2$ full cell and the image of lighted lamp driven by the full cell. (b) The typical charge-discharge profiles of the full cell between 0.6-3.6 V region at current density of 20 mA/g. (c) The cycle performance initial cycles and (d) the rate ability of the full cell

may be caused by the puckering [MoO_2] layers that accompanies the structural transformation. And the diffusion coefficient is about 7.3×10^{-11}-7.9×10^{-13} cm^2/s, which is considerably higher than other sodium-ion electrode material, indicating the potential for high rate application.[26, 27]

The assembling the full cell is an effective measure to investigate the application prospects of the electrode materials.[28-31] Thus a sodium-ion full cell is fabricated with the $Na_{0.3}MoO_2$ as the anode and $Na_{0.8}Ni_{0.4}Ti_{0.6}O_2$ as the cathode as shown in **Figure 4a**. The insert image in **Figure 4a** shows that LED lamps could be lighted successfully by the full cell. The charge-discharge curves of $Na_{0.8}Ni_{0.4}Ti_{0.6}O_2$ at a current density of 20 mA/g are displayed in **Figure S8**. $Na_{0.3}MoO_2$ // $Na_{0.8}Ni_{0.4}Ti_{0.6}O_2$ full cell is characterized using galvanostatic charge-discharge test at a current density of 20 mA/g in the voltage range of 0.6-3.6 V. The typical charge-discharge profiles of the full cell are illustrated as **Figure 4b**. A reversible discharge capacity of 80 mAh/g was obtained in the first cycle and subsequent cycles. Meanwhile the full cell exhibits a remarkable cycling performance as shown in **Figure 4c**, which offers 94.8% capacity retention for 100 cycles. The capacity decay of around 0.05% per cycle is measured. And the Coulombic efficiency is over 98% during the whole cycling. The rate ability of the full cell is also investigated at different current density of 20 mA/g, 50 mA/g and 100 mA/g as shown in **Figure 4d**. A reversible capacity of 57 and 38 mAh/g could be obtained at 50 and 100 mA/g respectively. When the current return to 20 mA/g, a capacity of 80 mAh/g could be remained, which suggest a good reversibility of the full cell. These favorable properties suggest that $Na_{0.3}MoO_2$ promises a capable anode for application in sodium-ion batteries.

Conclusions

In summary, a new layered molybdenum-based material, $Na_{0.3}MoO_2$, is synthesized by a solid-state method and the electrochemical performance of this material as an intercalation-type anode for sodium ion batteries is investigated for the first time. It displays a reversible capacity of around 146 mA/g with a safety average voltage of 0.8 V (vs. Na/Na^+) for sodium half-cell. In addition, the materials present excellent cycle retention and remarkable rate ability. The diffusion coefficients of this material are estimated to be 7.3×10^{-11}-7.9×10^{-13} cm^2/s. When it serves as anode in $Na_{0.3}MoO_2$ // $Na_{0.8}Ni_{0.4}Ti_{0.6}O_2$ full cell, the full cell presents an excellent cycling performance. The capacity retention of 94.8% is obtained after 100 cycles. We believe that the layered molybdenum-based oxide is a promising and capable anode material for sodium-ion batteries.

Notes and references

We thank Mr. Hailong Qiu and Miss Yuan Meng for the help with SEM and TEM. Kai Zhu is grateful for the financial support of the CSC (China Scholarship Council) scholarship. This work is supported by the 973 Program (No.251103).

1. B. Dunn, H. Kamath and J.-M. Tarascon, *Science (80)*, 2011, **334**, 928-935.
2. H. Pan, Y.-S. Hu and L. Chen, *Energy Environ. Sci.*, 2013, **6**, 2338-2360.
3. N. Yabuuchi, K. Kubota, M. Dahbi and S. Komaba, *Chem Rev*, 2014, **114**, 11636-11682.
4. M. H. Han, E. Gonzalo, G. Singh and T. Rojo, *Energy Environ. Sci.*, 2015, **8**, 81-102.
5. S. Guo, H. Yu, D. Liu, W. Tian, X. Liu, N. Hanada, M. Ishida and H. Zhou, *Chem. Commun*, 2014, **50**, 7998-8001.
6. W. Shen, H. Li, C. Wang, Z. Li, Q. Xu, H. Liu and Y. Wang, *J. Mater. Chem. A*, 2015. DOI:10.1039/C5TA03519H
7. X. Wu, W. Deng, J. Qian, Y. Cao, X. Ai and H. Yang, *J. Mater. Chem. A*, 2013, **1**, 10130-10134.

8. Y.-X. Wang, Y.-G. Lim, M.-S. Park, S.-L. Chou, J. H. Kim, H.-K. Liu, S.-X. Dou and Y.-J. Kim, *J. Mater. Chem. A*, 2014, **2**, 529-534.
9. S. Wang, W. Wang, P. Zhan and S. Jiao, *ChemElectroChem*, 2014, **1**, 1636-1639.
10. J. Y. Jang, Y. Lee, Y. Kim, J. Lee, S.-M. Lee, K. T. Lee and N.-S. Choi, *J. Mater. Chem. A*, 2015, **3**, 8332-8338
11. Z. Jian, P. Liu, F. Li, M. Chen and H. Zhou, *J. Mater. Chem. A*, 2014, **2**, 13805-13809.
12. X. Zhou, Z. Dai, J. Bao and Y.-G. Guo, *J. Mater. Chem. A*, 2013, **1**, 13727-13731.
13. H. Yu, Y. Ren, D. Xiao, S. Guo, Y. Zhu, Y. Qian, L. Gu and H. Zhou, *Angew. Chem. Int. Ed.*, 2014, **126**, 9109-9115.
14. S. Komaba, W. Murata, T. Ishikawa, N. Yabuuchi, T. Ozeki, T. Nakayama, A. Ogata, K. Gotoh and K. Fujiwara, *Adv Funct Mater*, 2011, **21**, 3859-3867.
15. S. Guo, H. Yu, P. Liu, Y. Ren, T. Zhang, M. Chen, M. Ishida and H. Zhou, *Energy Environ. Sci.*, 2015, **8**, 1237-1244.
16. K. Shen and M. Wagemaker, *Inorg Chem*, 2014, **53**, 8250-8256.
17. Z. Hu, L. Wang, K. Zhang, J. Wang, F. Cheng, Z. Tao and J. Chen, *Angew. Chem. Int. Ed.*, 2014, **126**, 13008-13012.
18. Y. Zhao, C. Han, J. Yang, J. Su, X. Xu, S. Li, L. Xu, R. Fang, H. Jiang and X. Zou, *Nano Lett*, 2015, **15**, 2180-2185.
19. R. McCarley, K.-H. Lii, P. Edwards and L. Brough, *J Solid State Chem*, 1985, **57**, 17-24.
20. R. Berthelot, D. Carlier and C. Delmas, *Nat Mater*, 2011, **10**, 74-80.
21. F. Sauvage, L. Laffont, J.-M. Tarascon and E. Baudrin, *Inorg Chem*, 2007, **46**, 3289-3294.
22. J. Xu, C. Ma, M. Balasubramanian and Y. S. Meng, *Chem. Commun*, 2014, **50**, 12564-12567.
23. P. J. Naeyaert, M. Avdeev, N. Sharma, H. B. Yahia and C. D. Ling, *Chem. Mater*, 2014, **26**, 7067-7072.
24. R. Shanmugam and W. Lai, *ECS Electrochem. Lett.*, 2014, **3**, A23-A25.
25. K. Zhu, H. Qiu, Y. Zhang, D. Zhang, G. Chen and Y. Wei, *ChemSusChem*, 2015, **8**, 1017-1025.
26. S. Guo, H. Yu, Z. Jian, P. Liu, Y. Zhu, X. Guo, M. Chen, M. Ishida and H. Zhou, *ChemSusChem*, 2014, **7**, 2115-2119.
27. Y.-B. Niu, M.-W. Xu, C. Cheng, S.-J. BAO, S. Liu, F. Yi, H. He and C. Li, *J. Mater. Chem. A*, 2015. DOI:10.1039/C5TA03127C
28. S. Xu, Y. Wang, L. Ben, Y. Lyu, N. Song, Z. Yang, Y. Li, L. Mu, H. T. Yang and L. Gu, *Adv. Energy Mater.*, 2015. DOI:10.1002/aenm.201501156
29. Y. Li, S. Xu, X. Wu, J. Yu, Y. Wang, Y.-S. Hu, H. Li, L. Chen and X. Huang, *J. Mater. Chem. A*, 2015, **3**, 71-77.
30. S.-M. Oh, S.-T. Myung, C. S. Yoon, J. Lu, J. Hassoun, B. Scrosati, K. Amine and Y.-K. Sun, *Nano Lett*, 2014, **14**, 1620-1626.
31. S. Guo, P. Liu, Y. Sun, K. Zhu, J. Yi, M. Chen, M. Ishida and H. Zhou, *Angew. Chem. Int. Ed.*, 2015. DOI: 10.1002/anie.201505215